JOURNAL OF MATERIALS SCIENCE 37 (2002) 2989–2996

Synthesis, characterization and photocatalytic property of nano-sized Zn_2SnO_4

WANG CUN*, WANG XINMING
Guangzhou Institute of Geochemistry, Chinese Academy of Sciences, Guangzhou 510640, People's Republic of China
E-mail: wangcun@gig.ac.cn

ZHAO JINCAI
Institute of Chemistry, Chinese Academy of Sciences, Beijing 100080, People's Republic of China
E-mail: jczhao@ipc.ac.cn

MAI BIXIAN, SHENG GUOYING, PENG PING'AN, FU JIAMO
Guangzhou Institute of Geochemistry, Chinese Academy of Sciences, Guangzhou 510640, People's Republic of China

Nano-sized Zn_2SnO_4 materials have been synthesized using the coprecipitation method. The synthetic conditions and the calcination behaviors of nano-sized Zn_2SnO_4 materials have been studied. The nano-sized Zn_2SnO_4 materials have been characterized with X-ray diffraction (XRD), transmission electron microscopy (TEM), thermogravimetry and differential thermal analysis (TG-DTA) and specific surface area. As a result, the kinetic grain growth equation for nano-sized Zn_2SnO_4 can be expressed as $D^{4.78} = 9.12 \times 10^{23} t \exp(-40.6 \times 10^3 / T)$, with an activation energy for grain growth of $Q = 337.9$ KJ/mol. The nano-sized Zn_2SnO_4 materials have been used as photocatalysts to decompose benzene in water solution. The results show that Zn_2SnO_4 can photocatalytically decompose benzene, and the photocatalytic capacity for Zn_2SnO_4 relates to the grain size, which is discussed in terms of the surface effect and the quantum size effect.

1. Introduction

Zn_2SnO_4 was first prepared by Coffeen with the wet method, and found to be an oxide semiconductor [1]; and its crystal structure was determined to be inverse spinel structure with the space group of $Fd3m$ by NBS [2]. Since then, Zn_2SnO_4 has received increasing attentions. Yoshida *et al*. had studied the preparation method and the growth conditions for Zn_2SnO_4 needle crystals, and observed that the needle crystals of Zn_2SnO_4 were grown at a fixed temperature of 1000 to 1300°C for 2 h from the vapor phase in a crucible using a starting mixture of ZnO powder and tin powder [3]. Chang *et al*. had studied the solid-state reaction system for SnO_2-ZnO, and observed that a solid-state reaction between SnO_2 and ZnO starts at up to about 1100°C, and Zn_2SnO_4 is the only resultant [4]. Scaife found that Zn_2SnO_4 has a photoelectrochemical effect, that is, a photoelectrochemical reaction can take place over a Zn_2SnO_4 anode under irradiation with proper wavelength [5]. Guillaumon *et al*. found that Zn_2SnO_4 may be used as coatings [6]. Zhang *et al*. observed that Zn_2SnO_4 has gas-sensitivities to reductive gases [7]. Chen *et al*. had studied the defect structure for Zn_2SnO_4, and suggested that the defect structure of Zn_2SnO_4 is Zn_2SnO_{4-x} with an *n*-type conducting property [8]. Gao *et al*. had studied that the humidity-sensing property for Zn_2SnO_4 [9]. Hashemi *et al*. had studied that the calcination behavior for Zn_2SnO_4 at higher temperature, and observed that the solid-state chemical reaction between SnO_2 and ZnO starts relatively slowly at about 1000°C to form Zn_2SnO_4, and the mono-phase, polycrystalline Zn_2SnO_4 formed when the mixture was fired at 1280°C for 12 h; and a calcination model had been suggested in which a diffusion-evaporation mechanism is responsible for the reaction between the SnO_2 and ZnO powders [10]. Wu *et al*. found that Zn_2SnO_4 may be used as the buffer layer for the CdS/CdTe photovoltaic heterojunction device [11]. Yu *et al*. had also studied that the electrical and gas-sensing properties for Zn_2SnO_4 [12, 13]. Belliard *et al*. used Zn_2SnO_4 prepared by mixing stoichiometric amounts of SnO_2 and ZnO and ball milling for 12 h and then calcining at 1000°C for 48 h, as an anode material for lithium battery [14]. The present study aims at the synthesis of nano-sized Zn_2SnO_4 with the coprecipitation method, and the explanation of the formation process for nano-sized Zn_2SnO_4 by the

*Author to whom all correspondence should be addressed.

characterizations of XRD, TEM, TG-DTA and specific surface area, then the evaluation of the photocatalytic activity for Zn_2SnO_4 to benzene. The results show that the nano-sized Zn_2SnO_4 can be synthesized with the coprecipitation method, and Zn_2SnO_4 exhibits photocatalytic activity to benzene. As a result, the kinetic grain growth equation of nano-sized Zn_2SnO_4 has also been formulated with the calculation of the activation energy for grain growth.

2. Experimental procedure

2.1. Preparation for nano-sized Zn_2SnO_4

The coprecipitation method was used to prepare the nano-sized Zn_2SnO_4. $SnCl_4 \cdot 5H_2O$ (Analytical reagent grade, or A.R.) and $ZnSO_4 \cdot 7H_2O$ (A.R.) were used as the starting materials, and NaOH (A.R.) as the coprecipitant without any further purification. $SnCl_4 \cdot 5H_2O$ and $ZnSO_4 \cdot 7H_2O$ in a 1 : 2 molar ratio were dissolved in a minimum amount of deionized water. Then the 4 mol/L NaOH solution was added to the above solution to adjust pH till about 7, and a white amorphous precipitate formed. The precipitate was filtered and washed with deionized water till no SO_4^{2-} and Cl^- were found after washing. Then the wet powders was isothermally dried at about 100°C in air, thus formed the precursor of Zn_2SnO_4. Finally the precursor was calcined in air to produce the nano-sized Zn_2SnO_4 materials.

2.2. Material characterization

The thermal decomposition behavior for the precursor of Zn_2SnO_4 was investigated using TG-DTA (Model CLT-2 thermogravimetric & differential thermal analyzer made by Beijing optical instrument factory) in air at a heating rate of 10°C/min. The identification of crystal structure and the calculation of average grain size were conducted from the XRD patterns taken on Rigaku D/max-1200 diffractometer operated at 40 kV, 30 mA and at the scanning speed of 4°/min. over the 2θ range from 10 to 60°, with Cu K_α radiation (Cu $K_\alpha = 0.15418$ nm). Particle size and morphology were observed by TEM (JEOL/JEM-1010) using an accelerating voltage of 100 kV. The specific surface area of Zn_2SnO_4 was measured by the gas sorption analyzer (Model NOVA 1000, Quantachrome Co.) with Brunauer-Emmett-Teller method (BET).

2.3. Photocatalytic experiment

Photocatalytic experiment was conducted using Zn_2SnO_4 to photo catalytically decompose benzene in water solution. The benzene is A.R. grade and used as supplied. The photocatalytic reactor consists of two parts: a 100 ml Pyrex glass bottle (sealed with a silastic plug) and a 125 W high pressure Hg lamp with a maximum emission at about 365 nm, which was positioned parallel to the Pyrex bottle. In all experiments, 0.50 g Zn_2SnO_4 materials were dispersed in 100 ml deionized water to form the suspensions, then 2 μl benzene was added to the above suspensions (so the concentration of benzene is 20 ppmv). The pH of suspension was not adjusted as it was. The suspension was magnetically stirred during irradiation, and to ensure the adsorption/desorption equilibrium, the suspension was magnetically stirred for 1 h before irradiation. The water samples were taken out at regular time intervals and benzene was measured by Tekmar 3000 Purge & Trap Concentrator followed by HP 5890/5970 Gas chromatography & Mass spectrometer (GC/MS).

3. Results and discussion

3.1. Phase and average size

Fig. 1a shows the X-ray diffraction patterns of the materials calcined for 10 h at different temperatures (500, 600, 700, 800 and 900°C). Fig. 1b shows the X-ray diffraction patterns of the materials calcined at 700°C for different times (2, 6, 10, 14 and 18 h).

The average grain size of Zn_2SnO_4 material can be determined from the broadening of the corresponding X-ray spectral peaks by Scherrer formula [15]:

$$D = \frac{K\lambda}{\beta \cos\theta} \tag{1}$$

where D is the average grain size, λ the wavelength of X-ray radiation, K usually taken as 0.9, and β the line width at half-maximum height after subtraction of equipment broadening. The average grain sizes of the Zn_2SnO_4 materials calculated from Scherrer formula are shown in Table I.

From Fig. 1a and b and Table I, it may be noticed that there is no change in crystal structure in the XRD pattern except these peaks continuously get sharper with increasing calcination temperature and calcination time. The crystal structures for all materials can be identified to be the inverse spinel phase of Zn_2SnO_4. From Table I, it can be seen that every material is nano-sized material with average grain size within the range of 1–100 nm [16], except the material calcined at 900°C for 10 h.

Fig. 2 shows that the TEM micrographs for the materials calcined for 10 h at different temperatures (500, 600, 700, 800 and 900°C).

The micrographs show that the Zn_2SnO_4 particles consist of uniform inverse spinel crystallites, and the morphology for material is homogeneous, and the distribution of grain size is narrow. The average grain size for Zn_2SnO_4 can also be approximately determined to be 3, 10, 25, 60 and 135 nm corresponding respectively to the material calcined for 10 h at 500, 600, 700, 800 and 900°C, respectively, which are in good agreement with those obtained from XRD patterns. A stronger agglomeration, which can be observed in the TEM micrograph for the material calcined at 600°C, especially 500°C for 10 h, can be attributed to the high surface energy of the nano-sized crystallites [17].

TABLE I Heat treatment condition and average grain size for Zn_2SnO_4

t_C (°C)	500	600	700					800	900
t (h)	10	10	2	6	10	14	18	10	10
D (nm)	3.0	9.7	17.4	22.8	24.3	26.0	28.0	59.3	134.7

Note: where t_C is calcination temperature; t is calcination time; D is average grain size.

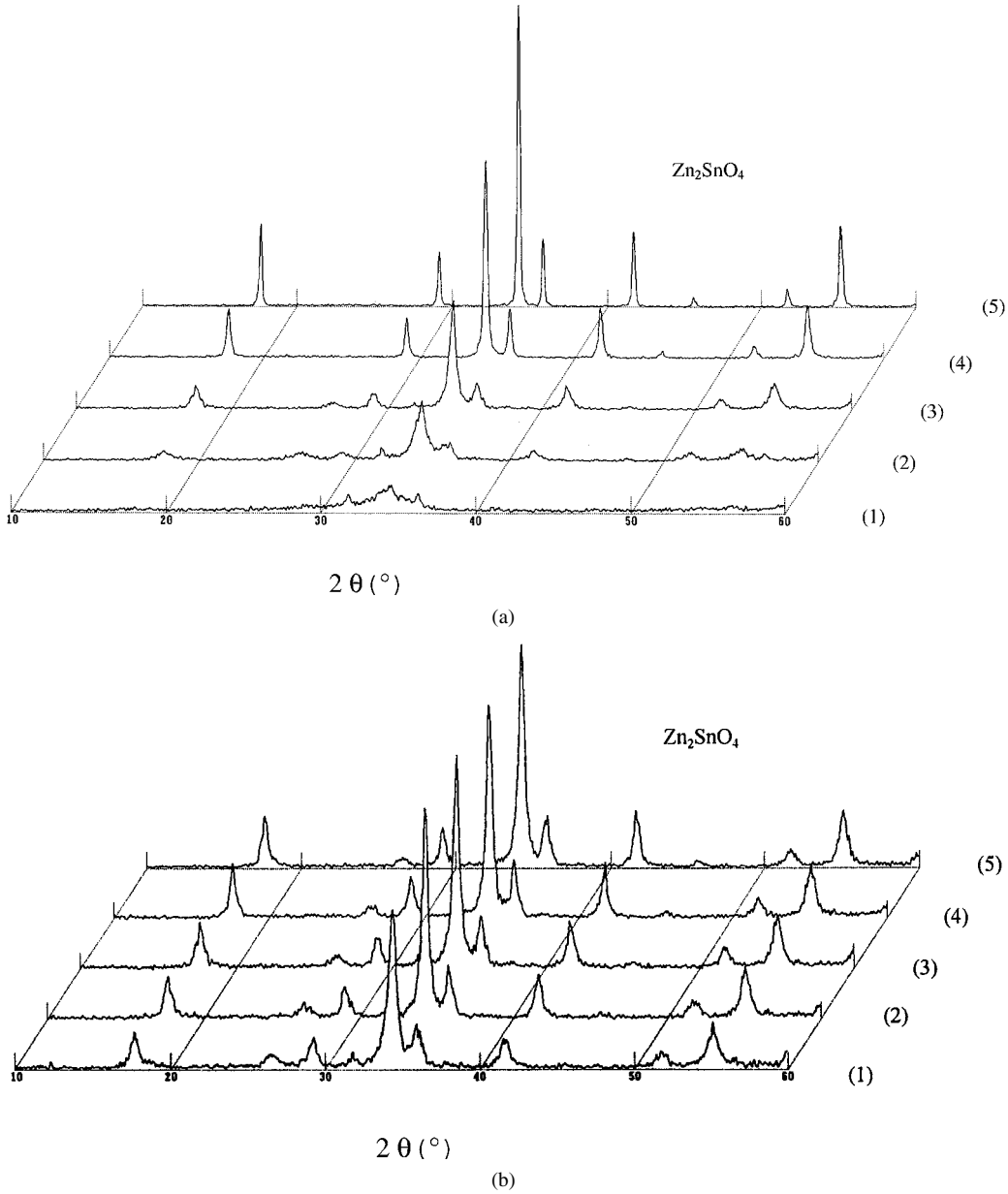

Figure 1 (a) XRD patterns of the Zn_2SnO_4 materials calcined for 10 h at: (1) 500°C; (2) 600°C; (3) 700°C; (4) 800°C and (5) 900°C; (b) XRD patterns of the Zn_2SnO_4 materials calcined at 700°C for: (1) 2 h; (2) 6 h; (3) 10 h; (4) 14 h and (5) 18 h.

3.2. Calcination behavior of nano-sized Zn_2SnO_4

Fig. 3 shows that the TG and DTA curves for the precursor of Zn_2SnO_4.

In the DTA curve, two endothermic peaks appear at about 86°C and 244°C, respectively, and an exothermic peak appears at about 724°C. In the TG curve, accordingly, a weight loss of about 5% in the temperature range of 41–129°C and another weight loss of about 5% in the temperature range of 208–292°C are observed, but no weight loss at about 724°C is observed. Combining the thermal analysis results with the results from XRD patterns, it can be suggested that the first endothermic peak in the DTA curve or the first weight loss in the TG curve might be attributed to the liberation of the surface-adsorbed water, and the second endothermic peak in the DTA curve or the second weight loss in the TG curve might be attributed to the liberation of the crystal water, and the exothermic peak of 724°C in the DTA curve might be attributed to the recrystallization of Zn_2SnO_4 [1].

The second weight loss of about 5% in the TG curve might be attributed to the following process:

$$Zn_2SnO_4 \cdot H_2O \rightarrow Zn_2SnO_4 + H_2O \qquad (2)$$

Pfaff obtained similar results while he studied the synthesis for Sr_2SnO_4 [17], Ba_2SnO_4 [18], Mg_2SnO_4 [19] and Ca_2SnO_4 [20]. Therefore, the reactions for formation of Zn_2SnO_4 can be summarized as follows:

$$\begin{aligned} 2Zn^{2+} + Sn^{4+} + 6OH^-(pH = 7) &\rightarrow 2Zn(OH)_2\downarrow \\ + Sn(OH)_4\downarrow &\rightarrow Zn_2SnO_4 \cdot H_2O \\ \rightarrow Zn_2SnO_4 + H_2O\uparrow & \end{aligned} \qquad (3)$$

The removal of the hydroxyl water occurred during the isothermal dry at 100°C.

Zn_2SnO_4 appears at about 244°C, which is significantly low compared with the temperature of about 1000°C for formation of Zn_2SnO_4 through the solid-state reaction between SnO_2 and ZnO powders

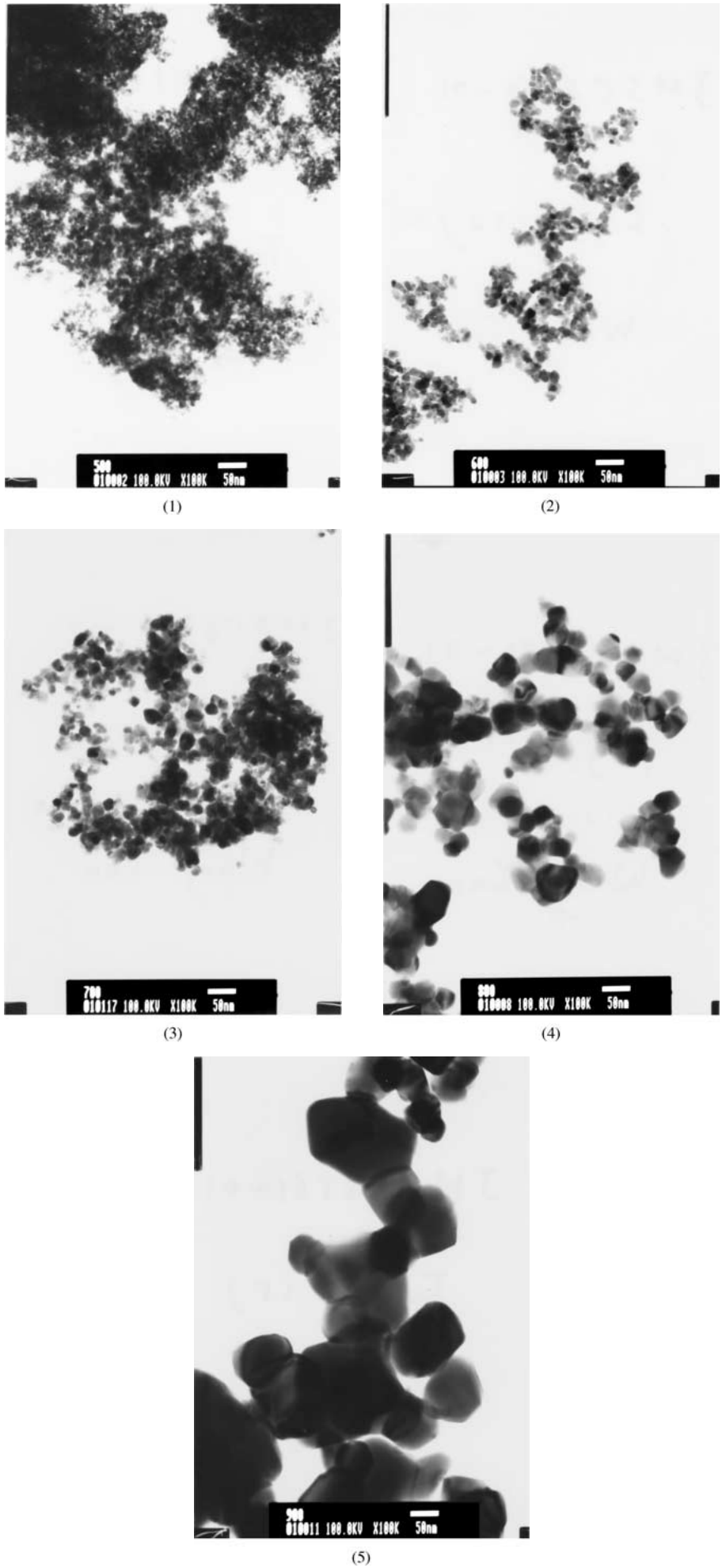

(1) (2) (3) (4) (5)

Figure 2 TEM micrographs of the Zn_2SnO_4 material calcined for 10 h at: (1) 500°C; (2) 600°C; (3) 700°C; (4) 800°C and (5) 900°C.

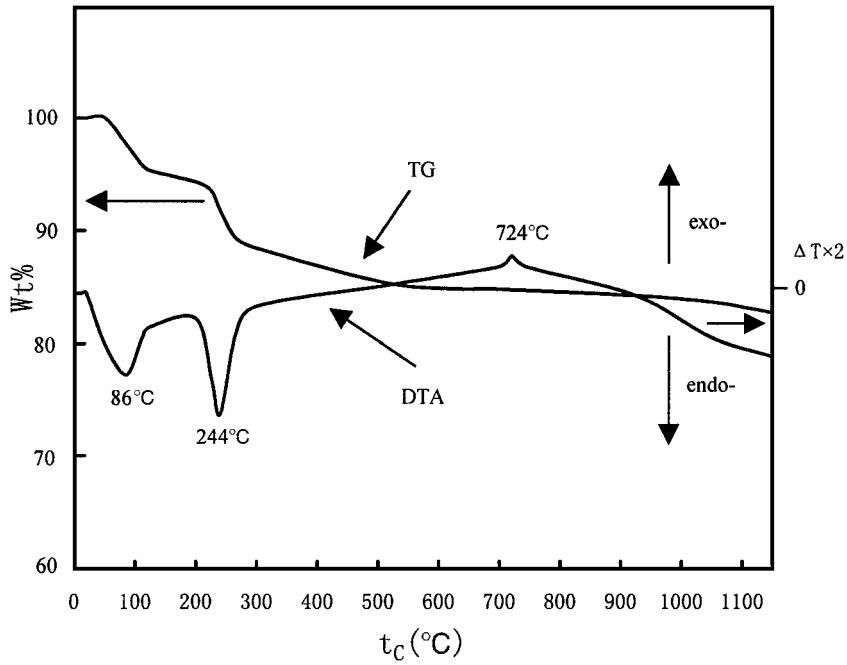

Figure 3 TG-DTA curves for the precursor of Zn_2SnO_4 (heating rate: 10°C/min. in air; temperature range: ambient to1150°C; sample weight: 40 mg).

[2, 10, 12, 13] or between Sn and ZnO powders [3]. From the TG and DTA curves, it can be seen that Zn_2SnO_4 is thermally stable so that no thermal decomposition take places till 1150°C. Yoshida *et al*. had observed that the Zn_2SnO_4 needle crystals can not be thermally decomposed at 1300°C [3], which is significantly different from another composite oxide $ZnSnO_3$ formed by ZnO and SnO_2. $ZnSnO_3$ can be thermally decomposed at about 700°C as follows [21]:

$$2ZnSnO_3 \rightarrow Zn_2SnO_4 + SnO_2 \qquad (4)$$

This reaction also suggests that Zn_2SnO_4 is more thermally stable than $ZnSnO_3$.

Li *et al*. found that the temperature for $La_{0.67}Sr_{0.33}MnO_3$ formation is about 900°C with the coprecipitation method compared with that of about 1350°C with the solid-state reaction method, and the former is significantly lower than the latter [22]. Li *et al*. [23], Hu *et al*. [24], and Lu *et al*. [25] obtained similar results, which can be explained as that the amorphous precipitates exhibit a loose bonding structure and do not require high activation energy for breaking bonds to generate new compounds [25]. In the present study, it is found that the minimum calcination temperature for formation of Zn_2SnO_4 with the coprecipitation method is about 756°C lower than that with the solid-state reaction between the SnO_2 and ZnO powders.

3.3. Activation energy for grain growth and kinetic grain growth equation for nano-sized Zn_2SnO_4

The following equation is usually used to express grain growth [26, 27, 28, 29]:

$$D^n - D_0^n = k_0 t \exp(-Q/RT) \qquad (5)$$

where D_0 is the initial grain size; D the grain size after a calcination of time t; n the kinetic grain growth exponent; k_0 a preexponential constant; Q the activation energy for grain growth; T absolute temperature; R gas constant.

Equation 5 has been successfully applied by Senda *et al*. to study grain growth of ZnO and ZnO-Bi_2O_3 ceramics [26], by Gülgün *et al*. to study grain growth of calcium aluminate [27], by Park *et al*. to study grain growth of $BaTiO_3$ [28], and by Kang *et al*. to study grain growth of the doped nano-sized ZnO [29], respectively. In the present study, the Equation 5 is also applied to study grain growth for nano-sized Zn_2SnO_4 calcined in the temperature range between 500 and 900°C.

In Equation 5, the initial grain size D_0, is usually negligibly small, so the Equation 5 can be given by:

$$D^n = k_0 t \exp(-Q/RT) \qquad (6)$$

From the slope of the $\ln D$ versus $\ln t$ line, which is $1/n$, the kinetic grain growth exponent n, is readily determined. Then the plots of $\ln D^n/t$ versus $1/T$ can be constructed and from the slope of the $\ln D^n/t$ versus $1/T$ line, the activation energy for grain growth Q, can also be readily determined.

Fig. 4a illustrates that the results of isothermal grain growth for nano-sized Zn_2SnO_4 calcined at 700°C.

From Fig. 4a, a kinetic grain growth exponent of 4.78 can be obtained.

Fig. 4b illustrates the temperature dependence of grain growth for nano-sized Zn_2SnO_4 calcined for 10 h. From Fig. 4b, an activation energy for grain growth of 337.9 kJ/mol can be obtained. The intercept of the line, which is $\ln k_0$, can be obtained to be 55.17, so $k_0 = 9.12 \times 10^{23}$. According to the above results, the kinetic grain growth equation for nano-sized Zn_2SnO_4 can be given by:

$$D^{4.78} = 9.12 \times 10^{23} t \exp(-40.6 \times 10^3/T) \qquad (7)$$

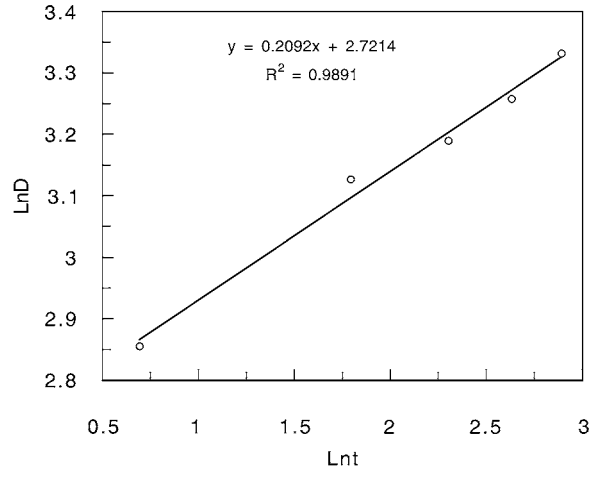

(a)

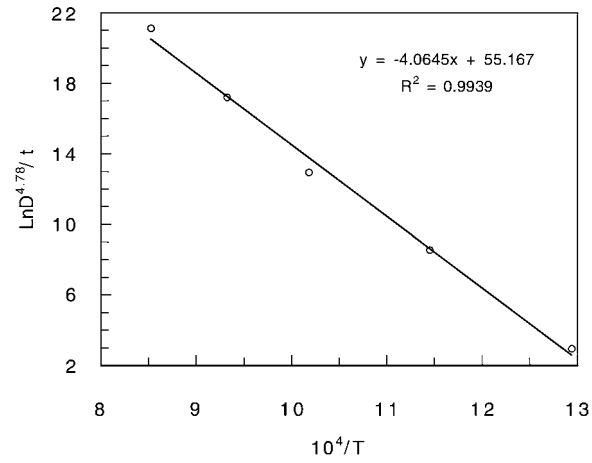

(b)

Figure 4 (a) $\ln D$ (grain size) versus $\ln t$ (calcination time) for the Zn_2SnO_4 material calcined at 700°C; (b) $\ln D^{4.78}/t$ versus $1/T$ for the Zn_2SnO_4 material calcined for 10 h.

3.4. Effect of the calcination temperature on the specific surface area for nano-sized Zn_2SnO_4

Fig. 5 shows that the BET specific surface areas for the Zn_2SnO_4 materials (S_{BET}) calcined for 10 h at different temperatures (500, 600, 700, 800 and 900°C).

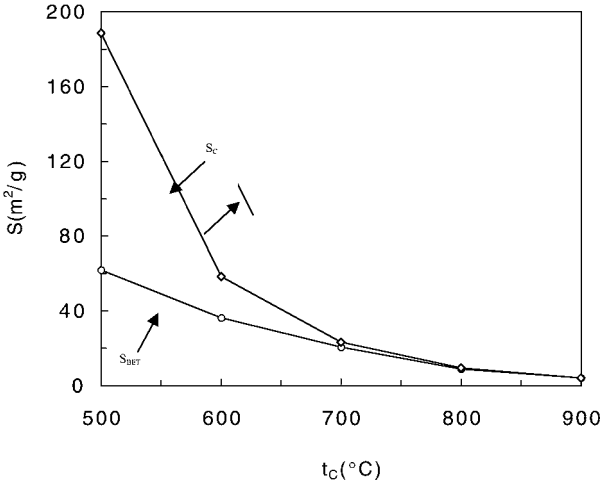

Figure 5 Correlation between the specific surface area (S) and calcination temperature (t_C) for the Zn_2SnO_4 material calcined for 10 h (S_{BET} is the BET specific surface area; S_C is the calculated value for specific surface area).

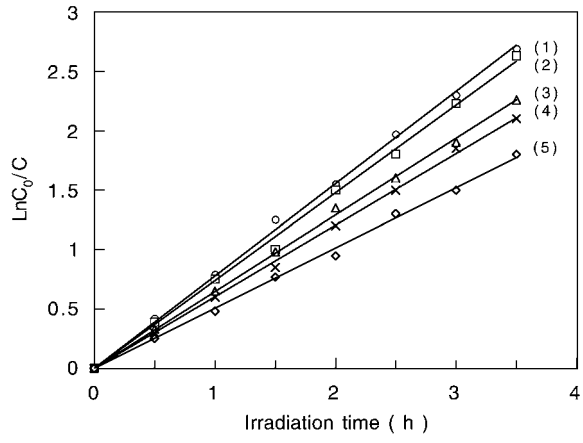

(a)

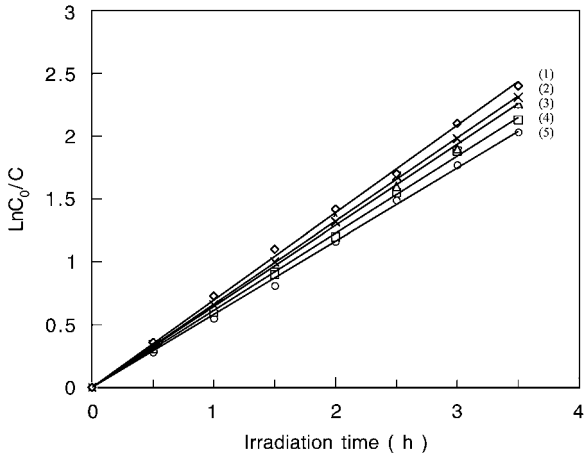

(b)

Figure 6 (a) Effect of the calcination temperature (for 10 h) on the photocatalytic activity for Zn_2SnO_4 to benzene ($C_0 = 20$ ppmv). Calcination temperature: (1) 500°C; (2) 600°C; (3) 700°C; (4) 800°C and (5) 900°C. (b) Effect of the calcination time (at 700°C) on the photocatalytic activity for Zn_2SnO_4 to benzene($C_0 = 20$ ppmv).Calcination time: (1) 2 h; (2) 6 h; (3) 10 h; (4) 14 h and (5) 18 h.

The S_{BET} of Zn_2SnO_4 material decreases significantly with increase in calcination temperature, which is due to increase in average grain size for Zn_2SnO_4 material with increase in calcination temperature.

It can be reasonably given that there is no agglomeration for the Zn_2SnO_4 material calcined at 900°C for 10 h, and thereby the mean size of the material particles can be thought to be 134.7 nm; and the absolute densities of Zn_2SnO_4 materials calcined at different temperatures a constant, so the specific surface area of Zn_2SnO_4 material can be calculated according to the formula [30]:

$$S = \frac{6}{\rho L} \tag{8}$$

where S is specific surface area, ρ absolute density, L mean size of particles.

The calculated results (S_C) are also illustrated in Fig. 5. It can be observed that the S_{BET} is in good agreement with the S_C for the Zn_2SnO_4 material calcined at 700°C and 800°C, respectively for 10 h, but the S_{BET} is about 62.43% and 32.82%, respectively of the S_C for the material calcined at 600°C and 500°C, respectively for 10 h, which might be attributed to the stronger agglomeration of the nano-sized crystallites calcined at 600°C, especially 500°C for 10 h.

TABLE II Relationship between calcination condition and rate constant value

t_C (°C)	500	600	700					800	900
t (h)	10	10	2	6	10	14	18	10	10
k (h^{-1})	0.7776	0.7383	0.6957	0.6627	0.6456	0.6136	0.5819	0.6021	0.5060

Note: where t_C is calcination temperature; t is calcination time; k is rate constant.

3.5. Photocatalytic property of Zn_2SnO_4

As the above mentioned, Zn_2SnO_4 is non-stoichiometry with the defect structure of Zn_2SnO_{4-x}. So when Zn_2SnO_4 is in equilibrium with O_2, the defect reaction take places as follows [8]:

$$2O_o \rightleftharpoons 2V_o^{\cdot\cdot} + 4e + O_2\uparrow \quad (9)$$

Therefore the electrons are produced, and thereby Zn_2SnO_4 is an n-type semiconductor. Chen *et al*. [8] had determined the band gap for the semiconductor E_g to be 3.4 eV. So the optical adsorption threshold for Zn_2SnO_4 can be calculated as follows [31]:

$$\lambda_g = 1240/E_g = 1240/3.4 = 364.7\ (\text{nm}) \quad (10)$$

which is within the UV range. So it is likely that Zn_2SnO_4 produces electron/hole pairs under irradiation by UV light with proper wavelength, and thereby shows photocatalytic property.

Fujihira *et al*. [32] and Turchi *et al*. [33] had studied that the photocatalytic decomposition behavior of benzene in water solution using TiO_2 as photocatalyst. In the present study, Zn_2SnO_4 has been used as photocatalyst to decompose benzene in water solution, and the results are illustrated in Fig. 6a and b.

It is observed from Fig. 6a and b that Zn_2SnO_4 can photocatalytically decompose benzene and the decomposition reaction is reasonably good consistent with the first order kinetics, which is expressed by the following expression:

$$\ln C_0/C = kt \quad (11)$$

where C_0 is the initial concentration of benzene, C the concentration of benzene after the reaction of time t, k the rate constant for photocatalytic reaction. The effect of calcination temperature or calcination time for Zn_2SnO_4 material on k value is showed in Table II.

Photocatalytic activity for a material has obvious relation to its specific surface area. Higher calcination temperature or longer calcination time will result in decrease in specific surface area that leads to decrease in photocatalytic activity of material [34]. From Fig. 6a, it can be seen that the photocatalytic activity of the Zn_2SnO_4 material calcined at 600°C, especially 500°C for 10 h is significantly higher than that of the rest materials, which might be attributed to the quantum size effect. When the size of nano-sized particles within the range of 1–10 nm, a quantum size effect might appear [31, 35, 36]. The quantum size effect results in broadening of band gap of semiconductor that leads to the electron/hole pairs having stronger reductive/oxidative ability, which thereby lead to increasing in photocatalytic activity [37].

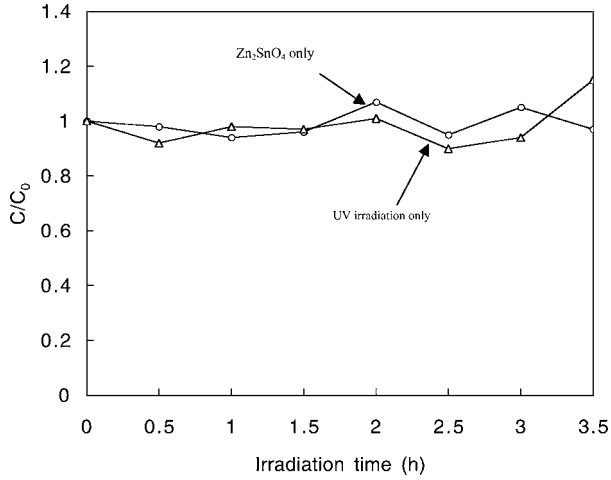

Figure 7 The results of blank experiment for photocatalytic activity of Zn_2SnO_4 to benzene ($C_0 = 20$ ppmv).

For comparison purposes, a blank experiment [38–40] has been conducted to determine that the variation of the benzene concentration under the reaction condition of Zn_2SnO_4 only or UV irradiation only. The results are illustrated in Fig. 7.

It can be observed that no variation of the benzene concentration occurs because the fluctuation in concentration ($\leq$15%) may be attributed to the instrumental error of measurement. A conclusion therefore can safely be made: Zn_2SnO_4 has photocatalytic activity to benzene. The reaction mechanism about photocatalytic decomposition of benzene needs to be further studied.

4. Conclusions

1. The nano-sized Zn_2SnO_4 can be synthesized using the coprecipitation method with proper reaction conditions. The synthetic process can be expressed by:

$$2Zn^{2+} + Sn^{4+} + 6OH^- \ (pH = 7) \rightarrow 2Zn(OH)_2\downarrow + Sn(OH)_4\downarrow \rightarrow Zn_2SnO_4 \cdot H_2O \rightarrow Zn_2SnO_4 + H_2O\uparrow$$

2. In the temperature range of 500 to 900°C, the activation energy for grain growth of nano-sized Zn_2SnO_4 is 337.9 kJ/mol, the kinetic grain growth equation for nano-sized Zn_2SnO_4 can be expressed by:

$$D^{4.78} = 9.12 \times 10^{23} t \exp(-40.6 \times 10^3/T)$$

3. Zn_2SnO_4 has photocatalytic activity to benzene under UV irradiation, and the photocatalytic activity relates to the grain size and the specific surface area for Zn_2SnO_4.

Acknowledgements

The authors wish thank Prof. H. Wang, Prof. Y. S. Shen and Prof. D. K. Peng of Department of Materials Science & Engineering of University of Science & Technology of China, and Dr. S. Wen, Prof. G. X. Wang, Prof. J. Q. Lei, Prof. F. Y. Wang, and Prof. G. X. Chen of Guangzhou Institute of Geochemistry for helps in this study. Support from the Natural Science Foundation of Guangdong province, China (Teamwork project "Environmental fate and control technology of the chemicals with adverse health effects in the Pearl River Delta") is gratefully acknowledged.

References

1. W. W. COFFEEN, *J. Amer. Ceram. Soc*. **36** (1953) 207.
2. NBS, Mono. 25, Sec. 10 (1972) p. 62.
3. R. YOSHIDA and Y. YOSHIDA, *J. Cryst. Growth* **36** (1976) 181.
4. L. L. Y. CHANG and R. C. KALDON, *J. Amer. Ceram. Soc*. **59** (1976) 275.
5. D. E. SCAIFE, *Solar Energy* **25** (1980) 41.
6. J. C. GUILLAUMON and L. J. C. BLET, *Demande FR* **2515** (1983) 673.
7. Z. T. ZHANG and Z. G. ZHOU, in Proc. of China-Japan Int. Sci. Symp. on Sensors, Harbin, People's Republic of China, 1986, edited by Y. S. Sheng, p. 95.
8. Z. Y. CHEN, Y. JIA, Z. D. ZHANG and Y. T. QIAN, *Journal of University of Science and Technology of China* **17** (1987) 343 (in Chinese).
9. N. F. GAO, H. Z. YU, X. F. ZHANG, Y. Y. LIU, Z. T. ZHANG and Z. T. ZHOU, *Journal of Inorganic Materials* **4** (1989) 125 (in Chinese).
10. T. HASHEMI, H. M. AL-ALLAK, J. ILLINGSWORTH, A. W. BRINKMAN and J. WOODS, *J. Mater. Sci. Lett*. **9** (1990) 776.
11. X. Z. WU, P. SHELDON and T. J. COUTTS, US Appl. 149, 430 (8 Sept. 1998) p. 32.
12. J. H. YU and G. M. CHOI, *Sensors and Actuators* B **52** (1998) 251.
13. *Idem*., *ibid*. **72** (2001) 141.
14. F. BELLIARD, P. A. CONNOR and J. T. S. IRVINE, *Solid State Ionics* **135** (2000) 163.
15. H. P. KLUG and L. E. ALEXANDER, "X-ray Diffraction Procedures for Polycrystalline and Amorphous Materials" (John Wiley and Sons, New York, 1974) p. 618.
16. P. BALL and L. GARWIN, *Nature* **355** (1992) 761.
17. G. PFAFF, *J. Mater. Sci*. **35** (2000) 3017.
18. *Idem*., *J. Eur. Ceram. Soc*. **12** (1993) 159.
19. *Idem*., *Thermochim. Acta* **237** (1994) 83.
20. *Idem*., *Mater. Sci. Eng*. B **33** (1995) 156.
21. S. Y. SHEN and J. S. ZHANG, *Sensors and Actuators* B **12** (1993) 5.
22. Y. D. LI, J. H. ZHANG, C. F. ZHU, W. LIU, Y. ZHOU and Y. T. QIAN, *Journal of Inorganic Materials* **12** (1997) 734 (in Chinese).
23. Y. D. LI, R. M. LIU, Z. D. ZHANG and C. S. XIONG, *Mater. Chem. Phys*. **64** (2000) 256.
24. M. Z.-C. HU, G. A. MILLER, E. A. PAYZANT and C. J. RAWN, *J. Mater. Sci*. **35** (2000) 2927.
25. C. H. LU and S. Y. LO, *Mater. Res. Bull*. **32** (1997) 371.
26. T. SENDA and R. C. BRAD, *J. Amer. Ceram. Soc*. **73** (1990) 106.
27. M. A. GULGUN, O. O. POPOOLA and W. M. KRIVEN, *ibid*. **77** (1994) 531.
28. E. T. PARK, *J. Mater. Sci. Lett*. **18** (1999) 163.
29. X. Y. KANG, T. D. WANG, Y. HAN, M. D. TAO and M. J. TU, *Mater. Res. Bull*. **32** (1997) 1165.
30. W. M. KEELY, *Anal. Chem*. **38** (1966) 147.
31. A. HAGFELDT and M. GRATZEL, *Chem. Rev*. **95** (1995) 49.
32. M. FUJIHIRA, Y. SATOH and T. OSA, *Nature* **293** (1981) 206.
33. C. S. TURCHI and D. F. OLLIS, *J. Catal*. **119** (1989) 483.
34. A. TOWATA, Y. UWAMINO, M. SANDO, K. ISEDA and H. TAODA, *NanoStruct. Mater*. **10** (1998) 1033.
35. L. BRUS, *J. Phys. Chem*. **90** (1986) 2555.
36. A. L. LINSEBIGLER, G. Q. LU and J. T. YATES, JR., *Chem. Rev*. **95** (1995) 735.
37. M. R. HOFFMANN, S. T. MARTIN, W. Y. CHOI and D. W. BAHNEMANN, *ibid*. **95** (1995) 69.
38. I. POULIOS and I. AETOPOULOU, *Environ. Technol*. **20** (1999) 479.
39. R. M. ALBERICI and W. F. JARDIM, *Appl. Catal*. B **14** (1997) 55.
40. J. C. ZHAO, T. X. WU, K. Q. WU, K. OIKAWA, H. HIDAKA and N. SERPONE, *Environ. Sci. Technol*. **32** (1998) 2394.

Received 23 April 2001
and accepted 28 February 2002